Electronic Supplementary Information

Nanosheet-based $Nb_{12}O_{29}$ hierarchical microspheres for enhanced lithium storage

Renjie Li,[ab] Xiangzhen Zhu,[b] Qingfeng Fu,[b] Guisheng Liang,[b] Yongjun Chen,[b] Lijie Luo,[b] Mengyao Dong,[c,e] Qian Shao,[d] Chunfu Lin,*[ab] Renbo Wei,[f,*] and Zhanhu Guo*[c]

[a] *Institute of Materials for Energy and Environment, School of Materials Science and Engineering, Qingdao University, Qingdao 266071, China.*

[b] *State Key Laboratory of Marine Resource Utilization in South China Sea, College of Materials and Chemical Engineering, Hainan University, Haikou 570228, China.*

[c] Integrated Composites Laboratory (ICL), Department of Chemical & Biomolecular Engineering, University of Tennessee, Knoxville, TN 37996, USA

[d] *College of Chemical and Environmental Engineering, Shandong University of Science and Technology, Qingdao, Shandong, 266590, China.*

e Key Laboratory of Materials Processing and Mold (Zhengzhou University), Ministry of Education; National Engineering Research Center for Advanced Polymer Processing Technology, Zhengzhou University, Zhengzhou 450002, China

[f] Research Branch of Advanced Functional Materials, School of Materials and Energy, University of Electronic Science and Technology of China, Chengdu, 611731, China

* *Corresponding authors. E-mail addresses: linchunfu@qdu.edu.cn (C. Lin), weirb10@uestc.edu.cn (R. Wei); zguo10@utk.edu (Z. Guo).*

Experimental section

Synthesis

Niobium chloride ($NbCl_5$, 3 mmol, 99%, Aladdin), oxalic acid dehydrate ($C_2H_2O_4 \cdot 2H_2O$, 15 mmol, 99.8%, Aladdin), and ammonium fluoride (NH_4F, 8 mmol, 99.99%, Macklin) were dissolved in deionized water (70 mL) and kept constant stirring for 30 min. This solution was then transferred to a Teflon-lined autoclave (100 mL) and maintained in an electric oven at 200 ^oC for 24 h. After the hydrothermal process, the obtained white precipitate was separated by centrifugation, washed with ethanol and ultrapure water, and dried in air at 80 ^oC. This dried specimen was calcined in air at 700 ^oC for 2 h to generate nanosheets assembled Nb_2O_5 hierarchical microspheres (n-Nb_2O_5). n-$Nb_{12}O_{29}$ was formed by calcining n-Nb_2O_5 at 750 °C for 12 h in a blended H_2/Ar (5/95%) atmosphere.

Characterizations

The X-ray diffraction (XRD) patterns of the materials were recorded on an X-ray diffractometer (Bruker D8). The microstructures, morphologies and chemical compositions were identified by high-resolution transmission electron microscopy (HRTEM, FEI Tecnai G2 F20), field emission scanning electron microscopy (FESEM, Hitachi S-4800), and energy-dispersive X-ray spectroscopy (EDX, JEM-ARM-200F). The N_2 adsorption–desorption isotherms were collected on a surface-area analysis instrument (Micromeritics ASAP 2020) to reveal the specific surface areas.

The working electrodes contained 65 wt% n-$Nb_{12}O_{29}$/n-Nb_2O_5, 25 wt% Super P® conductive carbon and 10 wt% polyvinylidene fluoride (PVDF) on copper plates. The electrolyte was composed of 1 M $LiPF_6$ in a mixture of ethylene carbonate (EC), dimethyl carbonate (DMC), and diethylene carbonate (DEC) at a volume ratio of 1:1:1. Two-electrode coin cells with the CR2016 type were assembled in an argon-filled glovebox containing the working electrodes, electrolyte, metallic lithium plates, and Celard 2325 microporous polypropylene separators. The mass loading of the active materials was ~1.4 mg cm^{-2}.

The galvanostatic discharging–charging experiments were performed using a battery tester (CT-3008, Neware) in a potential range of 3.0–0.8 V. The cyclic voltammetry (CV) and electrochemical impedance spectroscopy (EIS) measurements were accomplished by using an electrochemical workstation (CHI660E, Chenhua). The CV sweep rate varied from 0.2 to 1.1 mV s^{-1}. The EIS frequency ranged from 10^5 to 10^{-2} Hz.

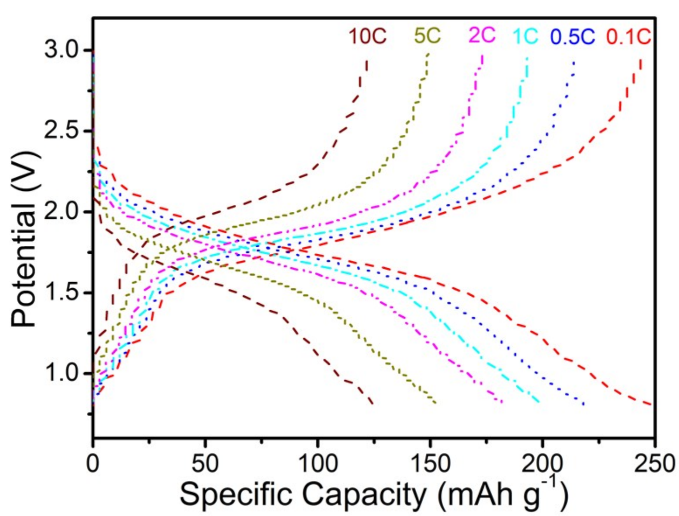

Fig. S1 Discharging–charging profiles of n-Nb_2O_5 at different current rates.

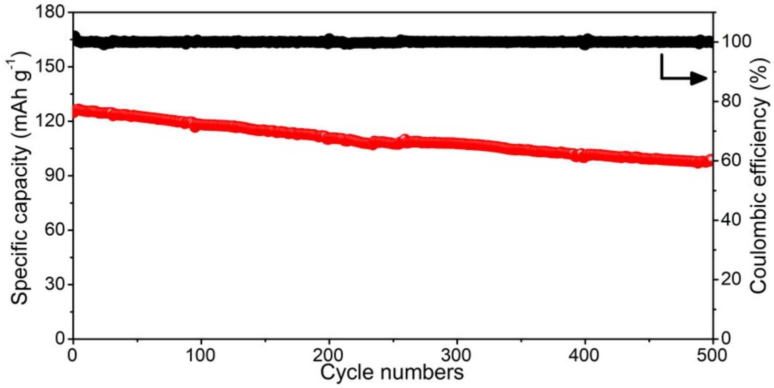

Fig. S2 Cycling stability of n-Nb_2O_5 at 10C over 500 cycles.

Table S1. Comparison of rate capability of n-$Nb_{12}O_{29}$ with previously reported niobium-based anode materials.

material	rate capability	reference
n-$Nb_{12}O_{29}$	179 mAh g^{-1} at 10C	this work
n-Nb_2O_5	125 mAh g^{-1} at 10C	this work
$Nb_{12}O_{29}$ micron-sized particles	165 mAh g^{-1} at 10C	[13]
$Nb_{25}O_{62}$ micron-sized particles	133 mAh g^{-1} at 10C	[13]
$W_5Nb_{16}O_{55}$ micron-sized particles	145 mAh g^{-1} at 10C	[12]
$W_{16}Nb_{18}O_{93}$ micron-sized particles	155 mAh g^{-1} at 10C	[12]
$GaNb_{11}O_{29}$ micron-sized particles	121 mAh g^{-1} at 10C	[21]
$GaNb_{11}O_{29}$ nanowebs	175 mAh g^{-1} at 10C	[21]
$FeNb_{11}O_{27.9}$ micron-sized particles	145 mAh g^{-1} at 10C	[22]
$Cr_{0.2}Fe_{0.8}Nb_{11}O_{29}$ micron-sized particles	123 mAh g^{-1} at 10C	[10]
$TiNb_6O_{17}$ micron-sized particles	178 mAh g^{-1} at 5C	[23]
$Ti_2Nb_{10}O_{27.1}$ micron-sized particles	180 mAh g^{-1} at 5C	[24]
$Ru_{0.01}Ti_{0.99}Nb_2O_7$ micron-sized particles	181 mAh g^{-1} at 5C	[25]
$Ti_{0.98}Nb_{2.02}O_7$ nanoparticles	120 mAh g^{-1} at 10C	[26]
$TiNb_2O_7$ nanofibers	137 mAh g^{-1} at 5C	[27]
$TiNb_2O_7$ nanorods	166 mAh g^{-1} at 10C	[14]
$TiNb_2O_7$ nanorods	154 mAh g^{-1} at 10C	[28]
$Ti_2Nb_{10}O_{29}$ porous nanospheres	179 mAh g^{-1} at 10C	[29]
$Ti_2Nb_{10}O_{29}$ hollow nanofibers	176 mAh g^{-1} at 10C	[30]
$Ti_2Nb_{10}O_{29}$/Ag composite	169 mAh g^{-1} at 10C	[31]